SEPTEMBER 2021 M.Sc. in Civil Engineering MOHAMMED SALAH QADER

REPUBLIC OF TURKEY

GAZİANTEP UNIVERSITY

GRADUATE SCHOOL OF NATURAL & APPLIED SCIENCES

FLEXURAL PERFORMANCE OF REINFORCED CONCRETE-ENCASED CONCRETE FILLED STEEL TUBES

M.Sc. THESIS

IN

CIVIL ENGINEERING

BY

MOHAMMED SALAH QADER

SEPTEMBER 2021

FLEXURAL PERFORMANCE OF REINFORCED CONCRETE-ENCASED CONCRETE FILLED STEEL TUBES

M.Sc. Thesis

in

Civil Engineering

Gaziantep University

Supervisor

Assoc. Prof. Dr. Mehmet Tolga GÖĞÜŞ

by

Mohammed Salah QADER

September 2021

I hereby declare that all information in this document has been obtained and presented in accordance with academic rules and ethical conduct. I also declare that, as required by these rules and conduct, I have fully cited and referenced all material and results that are not original to this work.

Mohammed Salah QADER

ABSTRACT

FLEXURAL PERFORMANCE OF REINFORCED CONCRETE-ENCASED CONCRETE FILLED STEEL TUBES

QADER, Mohammed Salah
M.Sc. in Civil Engineering
Supervisor:Assoc. Prof. Dr. Mehmet Tolga GÖĞÜŞ
September 2021
46 Pages

This study was presented to demonstrate how steel pipe beams behave with concrete CFST under pure bending, laboratory tests were performed on twelve test samples, which included two units of concrete CFST beam samples, a test that included ten sample units were classified into three groups It is as follows:

Two units of reinforced concrete with two different reinforcing diameters (8 mm, 12 mm) free of steel tube beam (control) as a control element. Four units of hollow steel tube were encapsulated with external reinforced concrete (control) with different reinforcing diameters (8 mm, 12 mm) and different thicknesses of the steel tube (1.5 mm, 3 mm) Hollow. The last four units En-cased (CFST) steel tube filled with control reinforced concrete containing different rebar diameters (8mm, 12mm) and steel tube with different thicknesses (1.5mm, 3mm), the important factors were relied on in this study. It is the nature of the use of the tube and the diameter of the rebar based on these parameters, the bending moment against the deflection in the mid-range and the deflection curves, the bending curves, the bending stiffness, the bending ability. Ductility was examined, and the results of the laboratory work showed a clear improvement in the instantaneous amplitude and strength of the CFST beams over Steel pipe beams filled with concrete. As confirmed by this study.

KeyWords: Concrete -Encased Concrete Filled Steel Tubes (CFST) Beams, Flexural Strength, Encased, Self-Compacting Concrete, Ductility.

ÖZET

BETONARMEYE GÖMÜLÜ IÇI DOLDURUKMUŞ ÇELIK TÜPLERIN EĞILME PERFORMANSININ INCELENMESI

QADER, Mohammed Salah
Yüksek Lisans Tezı, İnşaat Mühendisliği
Danışman: Doç. Dr. Mehmet Tolga GÖĞÜŞ
Eylül 2021
46 Sayfa

Bu çalışma, çelik boru kirişlerinin beton CFST ile saf bükülme altında nasıl davrandığını göstermek amacıyla sunulmuştur, iki birim beton CFST kiriş numunesini içeren on iki test numunesi üzerinde laboratuva testleri gerçekleştirilmiş, on numune birimini içerenbir test üçe ayrılmıştır. Gruplar aşağıdaki gibidir:

Kontrol elemanı olarak çelik boru kiriş (kontrol) içermeyen iki farklı donatı çapına (8 mm, 12 mm) sahip iki unite betonarme. Dört adet içi boş çelik boru, farklı takviye çaplarına (8 mm, 12 mm) ve farklı kalınlıklarda çelik boru (1.5 mm, 3 mm) Hollow'a sahip harici betonarme (control) ile kapsüllendi. Farklı inşaat demiri çapları (8mm, 12mm) ve farklı kalınlıklarda (1.5mm, 3mm) çelik boru içeren control betonarme ile doldurulmuş son dört adet En-kasalı (CFST) çelik boru, bu çalışmada önemli faktörlere güvenilmiştir. Borunun kullanımının doğası ve bu parametrelere gore donatı demiri çapı, orta aralıktaki sapmaya karşı eğilme momenti ve sapma eğrileri, eğilme eğrileri, eğilme sertliği, eğilme kabiliyetidir. Süneklik incelendi ve laboratuar çalışmasının sonuçları betonla doldurulmuş Çelik boru kirişlerine göre CFST kirişlerinin anlık genliğinde ve mukavemetinde açık bir gelişme gösterdi.

AnahtarKelimeler: Beton – Kaplanmış Beton Dolgulu Çelik Borular (CFST) Kirişler; Bükülme Mukavemeti; Kaplı; Kendiliğinden Yerleşen Beton; Süneklık.

''Dedicated to my family''

ACKNOWLEDGEMENTS

I would like to thank my supervisor,Assoc. Prof. Dr. Mehmet Tolga GÖĞÜŞ for his guidance and support throughout the study. I am thankful for his encouragement and motivation.

I would like to express my love and gratitude to my family and my parents for their support, always best wishes.

This work is supported by Bashar SHEHABand Abdulateef Saeed ABDULAZEZ, and Mustafa TAIFOR through the steps of the project, always best wishes.

TABLE OF CONTENTS

Page

LIST OF TABLES

Page

LIST OF FIGURES

Page

LIST OF SYMBOLS

$\mathbf{M_u}$	Moment Capacity
$\mathbf{D_u}$	Mid-span deflection at The Ultimate Moment
$\mathbf{D_I}$	Ductility Index
I	Moment of Inertia
$\mathbf{F_c}$	Strength of The Concrete
P	The Applied Force
T	Splitting Tensile Strength
L	Length of The Specimen
Ø	The diameter of Reinforced Steel in The Specimen
$\mathbf{D_y}$	Deflection at 0.6 ofThe Maximum Moment
$\mathbf{f_{sy}}$	Yield Strength of The Steel Tube
D	The Diameter of The Steel Tube
T	The Thickness of The Steel Tube
A	Width of The Specimen
B	Length of The Specimen
SCC	Self Compact Concrete

CHAPTER I

INTRODUCTION

This chapter presents a description of the encased CFST (Concrete-Filled Steel Tube) beams, then the application at which these beams were used. Finally, the thesis content is described.

1.1 General

Concrete-encased CFST coated members are widely used in tall buildings and bridges around the world due to their cost-effectiveness and advantages, including more confinement to primed concrete, higher hardness, improved durability and ductility, smaller section size, appropriate resistance Fire-retardant due to the presence of external control compared to bare CFST sections, preventing local torsion and corrosion of steel tube, and more suitable steel connections or control beams.

(An, et al. 2014) investigated the concrete-clad CFST efficiency, it was found that the bending capacity of the cross-section was a littleraisedin comparison withthe traditionalcontrol beams. The behavior of the load-deformation, bending ability, and initial bending stiffness were close to those of CFST beams. (Han, et al., 2014) performed an experimental and analytical investigation to find out the performance of large-scale concrete-coated CFST box members under the bending and presented that the bending performance of the concrete was developed by the designed design of the CFST box members.

Since the 1960s, Pre-stressed Concretemembers had been utilized in building structures and infrastructure installations because of their advantages like superior quality, more economic efficiency, shorter construction span, and extra-durable aesthetics (Nateghi, et al., 2018).

Concrete-filled steel tube (CFST) columns are increasingly used in composite construction. Under axial compression, the steel tube will sustain partial axial force and meanwhile provides the confinement to the infill concrete. The high axial strength capacity of CFST columns is largely related to the confinement provided by the steel tube. Extensive studies on CFST columns have been conducted. Nevertheless, how to quantify the efficiency of confinement effect in CFST columns using concrete with different strength grades is still missing. To address this issue, a series of compressive loading tests on CFST columns were conducted in present study. The variable parameters studied include concrete strength and diameter-to-thickness ratio of the steel tube. Six CFST stub columns in total were designed and tested under uniaxial compression. Axial strength, stress state in the steel tube, confined concrete strength and confining pressure acting on the infill concrete were carefully investigated. Test results show that the confinement factor (defined as the ratio of the nominal strength of empty steel tube to that of the unconfined concrete) is the most dominant factor influencing the confinement effect, and a larger confinement factor gives higher confinement effect. The low-strength concrete exhibits better performance of ductility and confinement compared with the high-strength concrete. The index of equivalent confining pressure was used to quantify the level of passive confinement provided by the steel tube in CFST columns. Based on the test results, a method to quickly quantify the confining pressure provided by the steel tube was proposed.

(Tuan, 2004) and (Christopher and Tuan, 2008) discussed the effect of post-stress on the behavior of bending in the circular steel tube sections filled with concrete. The results proveda significant rise in the capacity of the bending of the section.This raise is due to the exertion of post-tensile strength into the core of concrete (Deng, 2011). (Zhan, et al., 2016) indicated that prestressed strands can raise the effect of confinement on the concrete core subjected to bending, thus developing the performance of prestressed CFST beams in terms of strength, stiffness, and ductility.

In this study, a slight change is done to another study, by using different groups of lintels Reinforced concrete - steel tubes filled with concrete coated by the concrete of 76 mm in diameter and different thicknesses. The utilized groups are as follows:

The first group is a hollow steel tube surrounding the reinforced concrete.

The second group is an iron pipe surrounded from the outside with the reinforced concrete and filled with the inside with concrete.

1.2 Concrete-Filled Steel Tubes

Steel pipes filled with concrete are composite members, in which two different materials work together to support loads and provide rigidity. Generally, a tube filled with concrete is a round, rectangular, or square steel tube filled with concrete. The combination of steel and concrete in this way provides excellent flexural and axial capabilities and bending resistance. The steel tube also provides an excellent bonding of concrete which increases the compressive strength and compressive capacity of the accurate, which in turn increases the ductility of the organ. The total material weight of a traditional reinforced concrete structure can be much greater than the total weight of the material in a concrete-filled steel pipe structure with the same resistance. As a result of the lower weight of the building, the lateral forces that have to be designed will be less. In addition to the reduced overall weight, another benefit is the speed and ease of construction. The steel tube and framing elements can be constructed in the building several floors before concreting, as shown in Figure 1.2.

Figure 1.1 Concrete-encased CFST column with steel beams

1.3 Thesis Content

Chapter one presents and explains the purpose of using Encased CFST.

Chapter two shows the previous studies on the behavior of the Encased CFST.

Chapter three describes the experimental investigation about the CFST beams, and the effect of the inner tube on beam behavior encased CFST.

Chapter four describes the results were obtained from the influence of inner tube position and shape on encased CFST beam behavior. The outcomes identified in this chapter are discussed.

Chapter five presents the conclusions and the summary of this thesis based on the results of comparative investigations of this study with recommendations for future work.

CHAPTER II

LITERATURE REVIEW

In this chapter, the previous experimentallyinvestigations on the CFST columns and beams were presented in detail.

2.1 Literature Review About Encased CFST Members

(Li et al., 2016) proposed an investigational and analytical study about the behavior of the composite column under the effect of axial compressive. The experimental test involved 10 samples of concrete-encased CFST samples, two samples of reinforced concrete members as control, and four samples of CFST members as control also. The strength of concrete and the ratio of tube diameter to member diameter were the main parameters. The ductility, axial strain, and ultimate compressive strength were discussed accurately with the consider of parameter influences. The concrete confined by stirrups in addition to the steel tube was proposed and the stress against strain model was suggested by the FEA models. The results of the laboratory work were used for verifying the predictions. The stress development and the distribution of the internal forces were investigated accurately. The critical parameter effect was found out by parametric analysis. For predicting the ultimate strength, simplified methods were suggested. Figure 2.1 shows the circular concrete-encased CFST configuration.

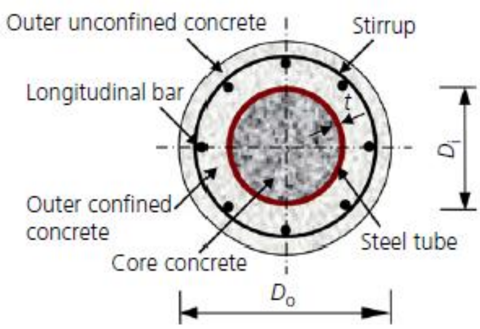

Figure 2.1 The circular concrete-encased CFST configuration(Li et al., 2016)

(El Basha et al., 2018) conducted a series of important laboratory works on nine samples of beams to discuss the flexural performance of various encased beams under the effect of bending and also to set apart the various failure manners. The samples were split into two groups, the first one was consisting of three rigid reinforced concrete beams while the second one was made of six hollow reinforced concrete encased tube beams. The major parameters' effect on the flexural performance of this kind of constructional member was determined. Six meters was the net span for all tested specimens. The reinforcement of the first beam CB1 that has a depth of 600mm was on the bottom side of it to be having the same depth of conventional reinforcing. The investigation focused on the beam depth decreasing the ability by utilizing steel tubes with consider keeping the same strength and stiffness. Reduction by 20% of the beam depth compared with the classical beam was an important aim of this study. A depth of 480 mm was used for the second sample CB2 with steel bars in the bottom region of the beam. The reinforcement and depth in samples B1 to B6 were identical to the CB2. Sample B7 had the same dimensions of B1 and B2 but, sample B7 had a classical reinforcement instead of the steel tube and had the same steel section area. After the testing and obtaining the results of this study, a useful and reasonable similarity was observed between the results of finite element analysis and the laboratory work. The hollow composite beam showed higher elastic deformation, higher ductility, and larger strength than the classical rigid reinforced concrete beam. Figure 2.2 shows a typical section of a hollow reinforced concrete-encased steel tube beam.

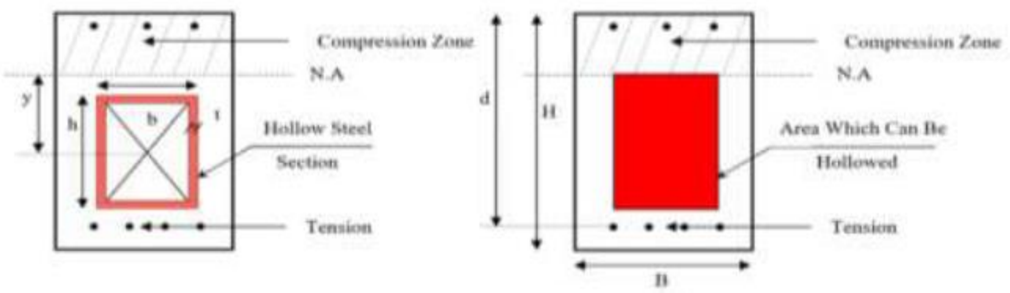

Figure 2.2 Typical section of the beams (El Basha et al., 2015)

(Yang et al., 2016) explained the influence of the earthquake represented by cyclic loading on the high-strength concrete-encased concrete-filled steel tube columns. Two conventional reinforced concrete columns and six high-strength concrete-encased concrete-filled steel tube columns were designed. Figure 2.3 shows the details of the specimens. Many behaviors related to earthquakes, like bearing capacity, ductility, stiffness, and energy dissipation were studied by using lateral displacement hysteresis curves. It was examined the influence of the prestressed steel strips layout and the arrangement of the stirrups on the composite columns' seismic performance. Compared with the classical columns, about 74.8% and 162.7%, respectively, were the increase in the energy dissipation and ductility performance of the high-strength concrete-encased concrete-filled steel tube columns. The composite columns' ductility was increased by 28.9%–63% as a result of the configuration of the prestressed steel strip, whereas the energy consumption performance was increased by 160.2%–263.3%. Finally, significant enhancement in bearing capacity, energy dissipation, stiffness, and ductility because of increasing the confinement that resulted from using prestressed steel strips and reducing the stirrup spacing of the concrete-filled steel tube columns.

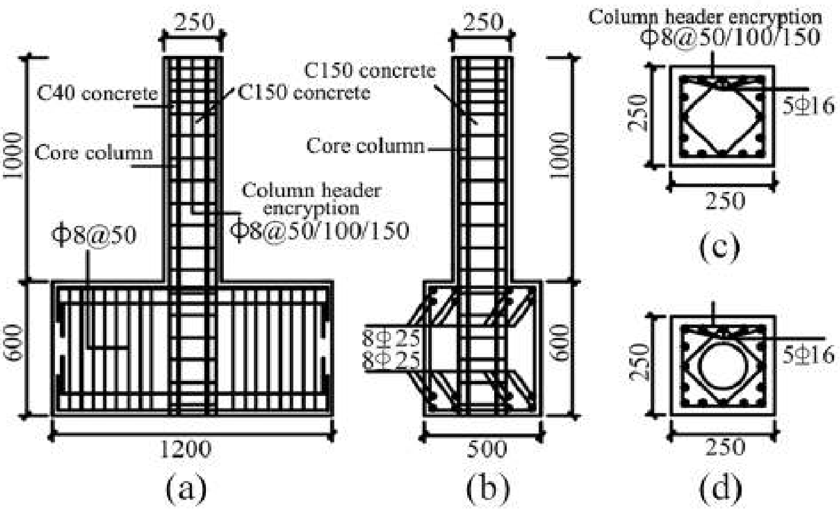

Figure 2.3 Specimen’s details: (a) façade, (b) side view, (c) column head and (d) composite column section(Yang et al., 2016)

(Cai et al., 2018) prepared a detailed study about the different mechanical behavior of outer concrete and inner CFST that led to crushing the external reinforced concrete in the concrete-encased CFST columns. The outer concrete was substituted with an engineered cementitious composite (ECC) that led to forming a new member of ECC-encased CFST columns. The final number was eleven samples of columns, seven of them were ECC-encased CFST columns while four of them were concrete-encased CFST columns. All specimens were subjected to a cyclic loading test. Figure 2.4 shows details of the ECC-encased CFST columns. Investigational results showed that the ECC-encased CFST columns were good from where cumulative energy dissipation and ductile stability were. The cumulative energy dissipation of ECC-encased CFST columns was twice compared with the concrete-encased CFST columns in addition to exhibiting stable ductile behavior. Also, the behavior of ECC-encased CFST columns were affected positively by increasing the stirrup ratio and the diameter of the steel tube.

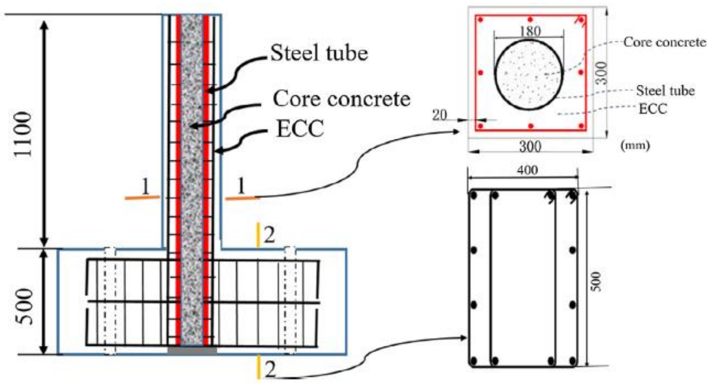

Figure 2.4 Details of the ECC-encased CFST column(Cai et al., 2018)

Zhou and Han (2018) studied the behavior of concrete-encased CFST members subjected to fire. Two specimens of cantilevered reinforced concrete beams and one specimen of continuous concrete-encased CFST column were the tested samples. The full-range fire and the influence of load were applied to specimens. The consecutive cooling phase, the loading stage at ambient temperature, the loading phase after the fire stage, and the fire exposure stage were the test procedure phases. The failure during post-fire loading and the failure during fire exposure were identified as kinds of failure. For all the column samples, global buckling was observed. The results of samples with common load showed good fire ratings without the need for extra fire protection. Also, the high post-fire residual resistance was the featured sign of concrete-encased CFST columns. Finally, the deformation during the cooling was significant as compared with that during the fire exposure stage.

Wang and Luo (2019) applied lateral cyclic loading on four samples of concrete-filled steel tube (CFST) columns and concrete-encased steel beams when the first three samples were prestressed while the fourth one was not prestressed. The test was showed the failure patterns of the samples and the distribution of cracks. Also, an accurate investigation was conducted about residential deformation, energy dissipation, ductility, and rigidity degeneration. Meanwhile, it was analyzed the strain difference kind of the I-steel flanges and longitudinal rebars at the beam end. For the three prestressed samples, the experimental results showed a bending failure at the ends of beams and a type of shear failure in the panel zone. For the non-prestressed sample, it was observed just bending failure at the beam ends. Also, good hysteretic performance was shown for all samples. Besides, the effect of the axial compression ratio on lateral loads was insignificant. It was discovered that the lateral maximum loads of prestressed samples could improve by lifting the prestress level. meanwhile, lifting the axial compression ratio and prestressing level could reduce the energy dissipation and ductility for the prestressed samples.

Lee et al. (2014) prepared a detailed study about the concrete-filled steel tubular columns encased with precast concrete. For examining the capacity of load-carrying, four specimens of columns that loaded by the eccentrical way and one specimen of columns that loaded concentrically were tested. Column length, eccentricity, and the PC cover reinforcement details were the test parameters. Increasing load-carrying capacity despite the small thickness of the cover precast concrete was observed. The cover concrete spalling of some samples was led to decreasing in the load-carrying capacity quickly after the overtaking of peak strength. The current design codes were used to calculate the predicted results and for doing a comparison between the peak strength and them.

2.2 Literature Review on The CFSTMembers

(Flor et al., 2017) proposed an investigational study to discover the behavior of large-scale CFST members when subjected to pure bending. Two various methods of casting were utilized to test two square hollow section specimens with twelvemetres length, while a pure bending test was carried out on six specimens with six meters length of square hollow section specimens. In the Structural Analysis laboratory, both of the two experimental tests were conducted. The first test included concrete pouring methods as major parameters, the cross-sectional type and the treatment methods of the steel-concrete interface were the major parameters of the second test. Basing on the laboratory work results, the relatively ductile mode was the behavior of rectangular CFST beams whereas the steel tubes' performance and the bending behavior were enhanced by the concrete infilling. Also, the results showed that the moment capacity of CFST members can predict by the rigid-plastic theory.

(Lachemi and Hossain, 2006) presented a comparison between the behavior of axially loaded steel tube columns filled with normal concrete and self-compacting concrete.A total of 16 columns with grade 450 for both normal cement and self-compacting concrete were tested by applying concentric axial load. Columns were without and with longitudinal and hoop reinforcement as well as tube confinement. The slenderness of the specimens was 4.8, 9.5, 3.1, and 6.5 for Series CI and Series CII, respectively. The ductility and strength of self-compacting concrete specimens were found similar to those of their normal concrete counterparts as the maximum strength enhancement in columns between 1.1% to 7.5% only. The presence of self-compacting concrete or normal concrete and the presence of hoop and longitudinal reinforcement had no significant influence on strain development.

Chitawadagi and Narasimhan in (2009) prepared research on the strength deformation behavior of circular steel tubes in-filled with concrete of different grades under bending. The actual effect of steel tube thickness, strength filling concrete, concrete cross-sectional area, concrete confinement, and moment capacity was investigated. The examined flexural strength is compared with the value prophesied by EC 4-1994, Load, and the AISC-1999. A group of 99 samples with all lengths of 1m was tested with concrete filling with characteristic strengths of 20, 30, and 40 N/mm^2 and a diameter to thickness ratio of 22.3 and 50.8. Based on the laboratory work results, interaction has been developed to foresee the curvature and moment of the Concrete Filled Steel Tube specimens. The results indicate that in the experimental investigation are used to all the hollow section resistance moments and the corresponding increase in curvature showed ductility better than the hollow. The ductility and moment of both the hollow and the CFST samples are increased by increasing the thickness of the tubes. For a given thickness of the concrete-filled steel tube specimen, rising the strength of the filled concrete will not help to significantly increase its capacity. The Strength Increase Factor (SIF) proposed here aids to estimate the concrete assistance to the moment capacitance of the concrete-filled steel tube beams. Detention of infill contributes to concrete to higher performance while higher strength infill concrete has been utilized for higher wall thickness steel tubes. Furthermore, EC 4-1994 foresees the moment capacity of the test samples moderately in the range of 30% to 35%. Since the influence of concrete filling is not taken into consideration and AISC-1999 is also the same, it is very conservative to predict the moment capacity of the concrete-filled steel tube section.

Chen et al. in (2021) carried out an experimental investigation on 10 stub column samples forextra verification of the applicability of the recommended design. The square and rectangular hollow tubes were produced by a combination of press-braking and welding. the important point was the strengths of steel and concrete used in this study exceeded the material's limits specified in EN 1994-1-1 standards. Two groups of steel plates with thicknesses of threeand six millimeters were utilized. Two types of concrete with cylinder strengths of 50 MPa and 90 MPa were used to fill the hollow tubes. Three coupons were removed from each group of steel. The average measured material properties are described in Figure 2.5. An overall experimental database consisting of 443 square and rectangular CFSTcolumns was collected, followed by a thorough statistical evaluationto find out the possibility of extending the current design equation in EN 1994-1-1 to the design of high strength square and rectangular CFST stub columns. Results of the statistical evaluations presented that the cross-section slenderness limit can be safely relaxed from $25\sqrt{\frac{235}{F_y}}$ to $68\sqrt{\frac{235}{F_y}}$. Also, it wasfound that the design equation could be extended to the design of the square and rectangular CFST stub columns.

Table 2.1 Test results of tensile coupons(Chen et al., 2021)

Steel	**E_s**	**N**	**f_y**	**f_u**	**ϵ_{sh}**	**ϵ_u**	**ϵ_f**
	GPa	**-**	**MPa**	**MPa**	**%**	**%**	**%**
3 mm	209.50	0.28	546.50	625.80	2.20	10.90	26.00
6 mm	213.30	0.28	580.70	666.10	2.30	10.10	25.40

2.3 Literature Review on FEA Investigations Of The CFST

(Rahmani et al., 2014) conducted a good laboratory test on six experimental samples of pre-stressed self-compacting concrete-encased CFST. The samples were divided into three divisions, the first one was made of four samples that involved pre-stressed strands for the tension region and CFST element for the compression region, the second one was consisting of one sample that involved pre-stressed strands without prestressing force and CFST element for the compression region. For the final sample, the tension region contained pre-stressed strands while the compression region lacked the CFST elements so six longitudinal bars replaced the steel tube. The diameter of both longitudinal bars and spiral stirrups was 8 mm, the space between every two stirrups was 200 mm. The diameter-to-thickness ratio for the steel tube, pre-stressing, and the eccentricity of the pre-stressed strand were the primary parameters of this test. Also, the ABAQUS finite element program was used for modeling 13 samples of high-strength prestressed concrete-encased CFST. Compressive cylinder strength of the concrete core, diameter to section width ratio for the steel tube, and yield strength of the steel tube were the main variables dependent on the FEA study. The FEA results were verified by the results obtained from the laboratory work. Figure 2.6 shows a comparison of failure manners between predicted and test specimens. It was confirmed that the effect of the outer concrete compressive strength on the flexural parameters was significant. Furthermore, the ultimate bending moment and serviceability flexural stiffness were increased minorly when the ratio of steel tube diameter to section width has increased, but the initial flexural stiffness was increasing significantly.

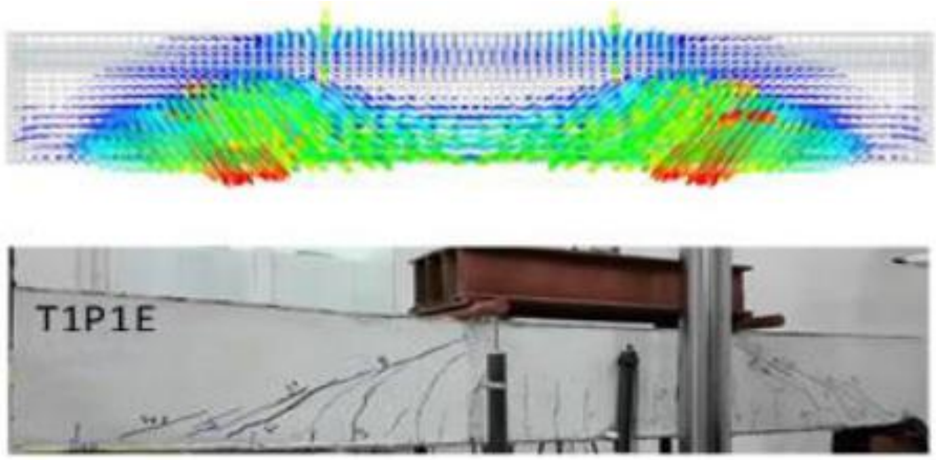

Figure 2.5 Comparison of failure manners (Rahmani et al., 2014)

Han et al. in (2015) utilized eight laboratory specimens for conducting some important tests on concrete-encased CFST, in addition to carrying out FEA. To investigate the effect of differences in the steel tube height (840 mm - 1260 mm) and diameter (74.9 mm - 102.2 mm) on the flexural behavior of concrete-encased CFST box members, six of the specimens were designed as concrete-encased CFST boxes while two of them were done as reinforced concrete box members. A detailed and accurate comparison of failure manners and flexural performance were conducted between concrete-encased CFST box specimens and the corresponding reinforced concrete box specimens. The influence of the shear-span-to-depth ratio, moment-curvature relation, and loading transfer was determined by the FEA model. For prophesying the flexural capacity of concrete-encased CFST box members, a simplified model was suggested as well as carrying out a parametric study depending on the FEA modeling.

A finite element analysis program (ABAQUS) to investigate numerically the mechanical performance of concrete-filled steel tube (CFST) columns. The numerical analysis of contact stress between the steel tube and the concrete showed a non-uniformly distribution of the contact stress under the effect of eccentric loading for the CFST column. Besides, it showed a primary difference with the CFST columns that were subjected to axial loading. Also, considering the effect of eccentricity, a new concrete model was proposed depicting the whole loading stages. The proposed constitutive model was validated by the existing experimental results employed for this purpose. It was found that the eccentric behavior of CFST columns could simulate by the proposed current model. Finally, the influences of concrete strength, steel tube ratio, and section steel ratio were checked under the eccentric loading for the CFST column (Cai et al., 2018).

Important investigational study that discussed the flexural behavior of concrete-encased by using concrete-filled steel tubes. To analyze the performance of this kind of composite beam, FEA models were advanced in addition to verifying the FEA modeling by a group of test data. All these access to simulations were conducted by the commercial program (ABAQUS). For describing the performance of the steel, the elastic-plastic model was used in this study. Poisson's ratio of steel utilized in this study was 0.3 while the elastic modulus was 206 000 N/mm^2. As related to concrete, the constitutive performance of concrete was described by applying the damage plasticity model. According to ACI 318-11, the modulus of elasticity for concrete was considered 4730 F_C'while the Poisson's ratio was considered 0.2. Three regions were the divisions of concrete for the composite section depending on the confinement conditions namely: inner concrete of the CFST, outer confined concrete, and outer unconfined concrete. Many analyses were carried out to investigate the true behavior of concrete-encased CFST such as stress distributions on the composite section, the interactions between concrete and steel, and the moment-curvature relation. The study showed that the thin-walled steel tubes can advance full plastic strength in the concrete-encased CFST beams without local buckling. Finally, the flexural capacity of concrete-encased CFST beams was calculated by simplified equations derived by a parametric study (An et al., 2014). Figure 2.7 shows a typical cross-section of concrete-encased CFST.

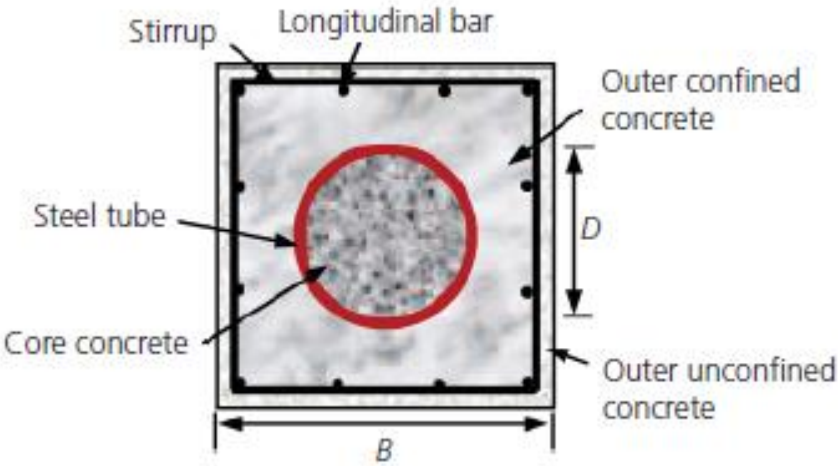

Figure 2.6 Typical cross-section of concrete-encased CFST (An et al., 2014)

Qian et al. in (2016) implemented an important study about the true performance of encased columns during applying side loading. The performance of this kind of composite constructional member was investigated by one of the finite element programs. The obtained results from the FEA program were compared with the predicted one with consideration to loading against displacement relationships, failure manners, and maximum strength. The accuracy of the FEA models was good and can replace the experimental results. The FEA models were used to analyze the relationships of loading-displacement, axial load allocation, and the stress resulting from the confined concrete inside the steel tube. Also, accurate comparison depended on the cyclic performance was conducted among the encased CFST column, classical CFST, and the reinforced concrete columns. Investigation of the effect of different parameters on the moment-curvature curves was carried out by utilizing parametric analysis. The axial loading ratio, the diameter of the tube to width ratio, the stirrup distinctive amount, the longitudinal steel bars ratio, the rate of steel for the inner

CFST, and the strength of the material. Finally, it was suggested a simple model for the moment-curvature relation of the encased column.

Chen et al. in (2020) tested twelve bending samples to find the performance of the encased CFST box beams through the effect of the section size, tube diameter, and bending direction. Then developed a numerical model to find out the flexural behavior of the composite beams. The test results were found that the outer RC component was deformed at the top while the inner CFST parts remained intact at mid-portion, as shown in Figure 2.8. The flexural cracks were distributed along the pure bending area uniformly. When the diameter of inner CFST increased, Mu increased about 27.6%–30.3% and the maximum width of vertical concrete cracks decreased. The parametric analysis presented thatM_u increased with respect tof_{ys}, $\alpha_{s,}f_{y1,}f_{cu,out}$&$\alpha_1$are increased, while there was a small influence of$f_{cu,core}$ onM_u. The increment in f_{ys}, $\alpha_{s,}f_{y1}$&α_1 might cause an increment of the residual moment. The simplified methods were used to predict the initial stiffness and the ultimate flexural strength.

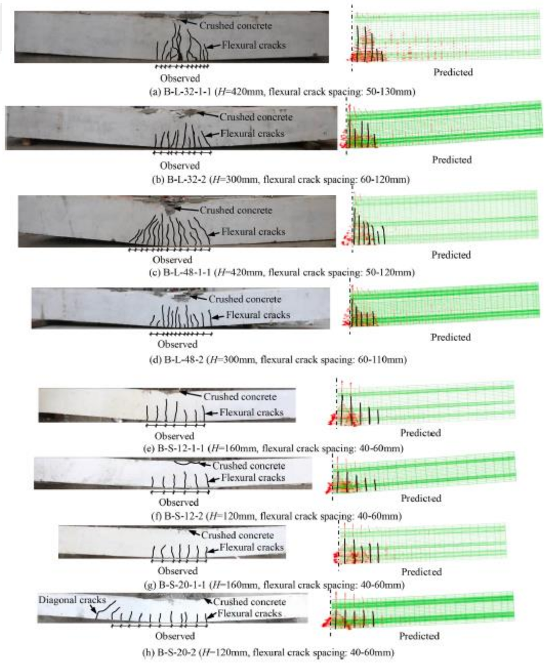

Figure 2.7 Failure modes of the tested specimens(Chen et al., 2020)

CHAPTER III

EXPERIMENTAL INVESTIGATIONS

In this chapter the designing of the specimens are described besides the experimental steps until the end of the tests.

3.1 Steps of The Experimental

In this chapter, the structural performance of CFST beams will be discussed. The study focused on the bending behavior through a group of 10 beams divided into three groups of four samples, the first is encased-CFST and four samples, the second is hollow, and the last two samples are steel tube beams filled with concrete and then compared these three groups of beams with a reinforced concrete beam which is the control beam. The samples are examined to measure the behavior in terms of the capacity of carrying the subjected loads. This chapter presents the specifications and properties of the elements used to construct and test samples.

3.2 Material properties

3.2.1 Self-Compacted Concrete (SCC)

In this study, the mixing ratio of (SCC) consisted of cement, fly ash, water, superplasticizers, natural fine aggregates with maximum particle sizes of 4 mm, and pulverized sand with a range of particle sizes ranging from 0.3 mm to 2 mm, and less than 0.3 mm as overallfine with maximum 10 mm particle sizes are used as shown in Table 3.1 and Figure 3.1. Fly ash and superplasticizers are used to increase workability. The mixture is designed to a grade of 40MPa and the water to cement ratio of 0.33 and the mixing ratio of the self-compacting concrete is used below.

Table 3.1 Properties of the mixed design

Density(kg/m^3)	Cement(kg/m^3)	Fly ash(kg/m^3)	Water(kg/m^3)	Superplasticizer (kg/m^3)	Coarse aggregate(kg/m^3)	River sand(kg/m^3)	Crushed sand(kg/m^3)
2338.27	285	285	188.1	2.77	709.83	650.678	216.893

Figure 3.1 Mixing of the SCC

The durability of concrete was a major concern in Japan. Conventionally, construction of durable structures commands for adequate concrete compaction by the skilled personnel. The gradual decline in the number of skilled personnel in Japan's construction industry lead to a reduction in construction works quality. For this, an innovative self-compacting concrete was developed with the aim of producing durable concrete units independent of the quality of the ongoing construction work.

The properties and specifications of concrete were determined from standard cylindrical tests. Twenty precise concrete cylinder tests were carried out. The average compressive and the strength of the mixture ratio was determined in the laboratory on the day of testing on eight cylinders of 100 mm by 200 mm as shown in Figure 3.2. The average compressive strength of concrete was 49.446 MPa while the average tensile strength to split was 10.05 MPa. The concrete cylinder samples were tested based on the ASTM C39 / C39M standard. Equation 3.1 is used to calculate the splitting tensile strength (T), where (P) represents the maximum applied load measured in N, the symbol (L) represents the length of the specimen measured in mm, and the symbol (D) refers to the diameter of the specimen measured in mm.

$$T = \frac{2 \times P}{\pi \times L \times D} \quad \text{...(3.1)}$$

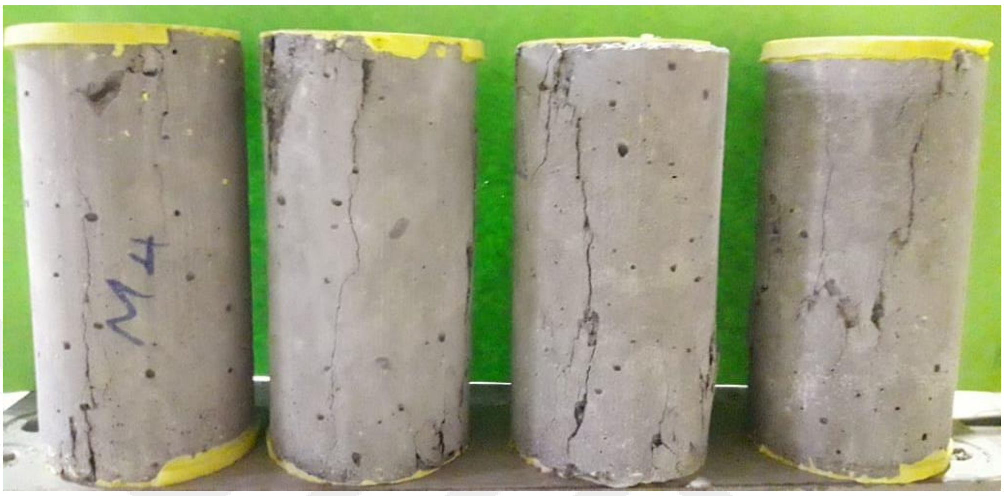

Figure 3.2 Concrete cylinders after testing

SCC attains remarkable compaction by using its own weight and without necessitating for mechanical vibration. This state of the art material was first proposed by Okamura in 1986 [59].

According Aitcin [61], High-Performance Concrete may be referred to as concrete with high durability and with relatively low-water cement ratio. For this, the use of high performance concretes has found widespread applications in delivering high durability concrete.

High-Performance (SCC) is well known as concrete with good deformability. SCC can be used to fill closely reinforced areas without the need for mechanical vibrations. Additionally, SCC has very high resistance to particle segregations. To achieve outstanding self-compact ability, especially in highly reinforced areas, SCC should deform appropriately without segregating its components. Slump flow test can be used as the evaluation test for estimating the deformability of SCC under its own weight.

Self compacting concrete (SCC) can be defined as fresh concrete that flows under its own weight and does not require external vibration to undergo compaction. It is used in the construction where it is hard to use vibrators for consolidation of concrete.

The (SCC) is also known as self-consolidating concrete, is characterized by its high fluidity. Thanks to this property, it spreads into concrete formwork with no need for vibration equipment. This non-segregating concrete is distributed by its own weight, while maintaining the properties of regular concrete, such as durability and strength.

Some of (SCC) mixtures include admixtures like superplasticizer and viscosity modifiers to reduce bleeding and segregation. When concrete segregates, it loses strength and results in honeycombed areas throughout the surface. However, a well designed self-compacting concrete will not segregate thanks to its plasticity and stability.

3.2.1.1 Applications of (SCC)

The self-compact concrete is mainly utilized in the following applications:

1. Construction of raft and pile foundations.
2. Retrofitting and repairing constructions.
3. Structures with complex reinforcement distributions.
4. Construction of earth retaining systems
5. Drilled shafts and columns.

3.2.1.2 Where Are Used SCC Self Compact Concrete

As per the below area used Self Compact Concrete.

- Better surface finish.
- Easier placing.
- Faster construction.
- Greater freedom in design.
- Improved durability.
- Reduced noise level.
- Reduction in site human resources.
- Safer working environment.
- Thinner concrete sections.

3.2.2 Current Advancement And The Pros And Cons Of Self-Compacting Concrete.

Self-compacting concrete (SCC) plays a significant role in the construction industry in these modern times where cost-effectiveness and time constraints are of principal concern.

Researchers are surveying all possible concentrations and properties of SCC relating to a country's development and advanced technology worldwide.

SCC is a ground-breaking building material which is broadly regarded as one of the most meaningful technological innovations in the concrete industry. Its inherent characteristics and ability to flow under its weight is creating numerous opportunities that would otherwise not be possible with regular concrete.

SCC is fundamentally an extension of standard concrete technology, providing comparable or advanced engineering properties while offering higher plastic performance. To achieve its stand-out performance features and flow-ability, a significantly larger cementitious constituent is needed to provide higher paste content. Also, the water-to-concrete ratio of the mixtures are low, therefore necessitating a higher dosage of polycarboxylate-based, high-range water lowering admixtures to attain workability and fluidity. In some cases, lethargic mineral fillers like limestone powder, and viscosity modifying admixtures are implemented to upsurge the stability of the mixture or forbearance to segregation.

3.2.2.1 Advantages of (SCC)

The SCChas several advantages in comparison with ordinary concrete. Some of these benefits are:

1. Quick placement without mechanical reinforcement.
2. Improved constructability.
3. Reduces permeability in concrete structures.
4. Reduces voids in highly-reinforced areas.
5. Eliminates problems associated with concrete vibration.
6. Creates high quality structures with improved structural integrity.
7. High durability, strength and reliability.

8. Reduction in labor costs.
9. Since it can be used in complex forms, it permits for innovative architectural properties,.
10. produces smoother and more aesthetic surface finishes.
11. Permits easier pumping, and there are many placement techniques available.

3.2.2.2 Disadvantages of (SCC)

As with any construction material, self-compacting concrete (SCC) faces the following limitations:

1. Material selection is more strict.
2. Construction costs increase, compared with regular concrete.
3. Many trial batches and laboratory tests are required to use a designed mixture.
4. Higher precision is required when measuring and monitoring.
5. There is no internationally accepted test standard for self-compacting concrete (SCC) mix.

3.2.2.3 Material Use In (SCC) Self Compacting Concrete.

As below material used in (SCC) Self Compacting Concrete.

• Cement.
• Aggregates.
• Mixing Water.
• Chemical Admixtures.
• Mineral Admixtures.
• Fly Ash.
• Ground Granulated Blast Furnace Slag Ground Granulated Blast Furnace Slag (GGBFS).
• Silica Fume.
• Stone Powder.
• Fibres.

3.2.2.4 Special Considerations When Using (SCC)

When using this type of concrete, there are several special considerations to achieve the best results. First of all, the production of self-compacting concrete (SCC) requires more experience and care than regular vibrated concrete. Also, the formwork used must be designed to withstand a higher pressure than with regular concrete. Finally, using mixers at full capacity is not recommended due to the high fluidity of self-compacting concrete (SCC) - it may spilled along the road, causing contamination.

3.2.3 Steel Tubes

This study included a beam of a concrete steel tube coated with light steel tubes with circular shapes for the inner tubes, where the nominal diameter of the steel tube was 76 mm and the nominal thicknesses of the tubes used were 1.5 mm and 3 mm. Tension coupons were taken from all faces except for the face welded in the tube to avoid unequal energy due to welding. Tensile strength tests were performed and tested according to the recommendations of ASTM E8 / E8M-15a (2015) (ASTM E8 / E8M-15a, 2015) illustrated in Figure 3.3.

Figure 3.3 Tensile specimens

3.2.4 Specimen's Properties

A total of eight units of composite beams are prepared and ready for laboratory testing which includes four hollow samples containing an inner steel tube, the other four encased specimens, reinforced concrete traction samples (control), and traction units of CFST concrete-filled steel tube beam and a conventional tube girder Filled with concrete. CFST packages have been categorized into three groups. Test sample totals were divided according to the thickness of the inner tube and the diameter of the armature used. The steel tube diameters and thicknesses for each sample are listed in Table 3.2 and Figure 3.4 shows full details. Reinforced concrete was placed in molds made of plywood with a thickness of 21 mm and dimensions of 150 x 150 x 820 mm, where the mold was closed from the bottom of the same material as at the top and left open for the purpose by filling the mold with concrete through and then pouring self-pressure concrete into the tubes steel from above without any pressure, as shown in Figure 3.4. The steel rods with a diameter of 6 mm and a distance of 7.5 mm were used as the main reinforcing 8 mm and 12 mm, and a steel tube of 76 mm in diameter with different thicknesses 1.5 mm and 3 mm was added in the center of the beams as shown in Figure 3.5. Figures 3.6 and 3.7 describe extra steps of the experimental procedure.

Figure 3.4 The specimens during casting

Figure 3.5 The specimen before casting (front view).

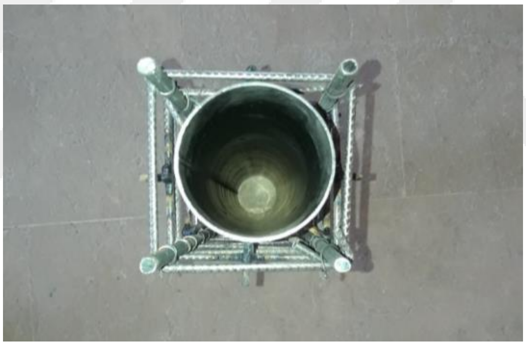

Figure 3.6 The specimen before casting (top view)

Figure 3.7 The inner part of the specimen

Table 3.2 The details of the Specimens

Group name	Specimen label	D*t in (mm)	a*b in (mm)	Ø in (mm)	f_{sy} in (MPa)	F_c in (MPa)
Control Group	C8	-------	150*150	8.00	------	49.52
	C12	-------	150*150	12.00	------	49.52
First Group	H8 t1.5	76.10*1.50	150*150	8.00	256.50	49.55
	H12 t1.5	76.10*1.50	150*150	12.00	365.36	49.55
	H8 t3	76.10*3.00	150*150	8.00	256.50	49.55
	H12 t3	76.10*3.00	150*150	12.00	365.36	49.55
Second Group	E 8 t1.5	76.10*1.50	150*150	8.00	323.33	49.28
	E12 t 1.5	76.10*1.50	150*150	12.00	293.73	49.28
	E8 t3	76.10*3.00	150*150	8.00	323.33	49.28
	E12 t 3	76.10*3.00	150*150	12.00	293.73	49.28
Third Group	CFST t1.5	76.10*1.50	-------	-	270.36	49.50
	CFST t3	76.10*3.00	-------	-	333.34	49.50

In Table 3.2, the dimensions of the specimens are described and classified into three groups. The state of the ray sample. For example, the classification "H8 t1.5" describes the following sample:

- "CFST" means concrete-filled steel tube.
- The "Hollow" mark means that the steel tube does not contain concrete.
- The "Encased" mark means that the steel tube is filled with ordinary concrete.

- The symbol "C" means that it is free of steel tube and is hollow in the center of the sample.
- The numbers "8 mm and 12 mm" denotes the diameter of the main rebar.
- The symbol "t" indicates the thickness of the steel tube.

Figure 3.8 The specimens after casting

After the curing period, if any shrinkage occurs, the gap is filled with epoxy and then covered with a steel plate. With another 3 mm thickness by welding, and finally, samples are prepared for testing as shown in Figure 3.9.

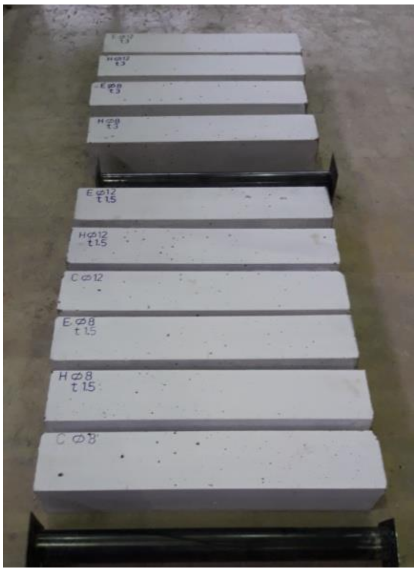

Figure 3.9 The specimens prepared to test

3.3 Test Procedure

Beams are tested by using a 500 kN bending test machine. All beams are tested under simply supported end conditions and under four-point loading with (1 mm/min) displacement control loading method. Since the structure is held at a distance of 820 mm from both ends of the beam, the net span is (750 mm). Four-point loadings are approved for testing and provides a net bending zone of 250 mm at the center of the specimen. The axis of the sample is carefully aligned with the axis of the loading device. Three LVDT (linear variable differential transformers) are fixed with beam length and deflection measurement. Of the three LVDT, two are at (175 mm) on both sides of the mid-range, and the third is center precisely mounted in the mid-range. All packages are subjected to failure. Figures 3.10 and 3.11 describe the flexure test effect on the reinforced concrete-encased CFST beam before and after loading respectively. Figure 3.12 describes a schematic diagram of the LVDT locations.

Figure 3.10 The specimen before loading

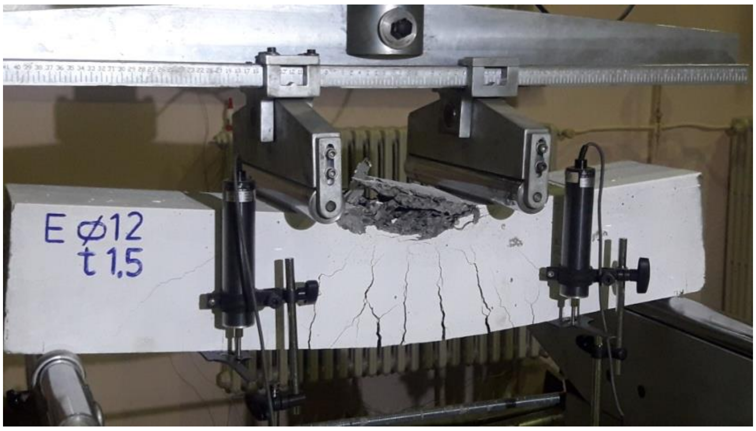

Figure 3.11 The specimen after loading

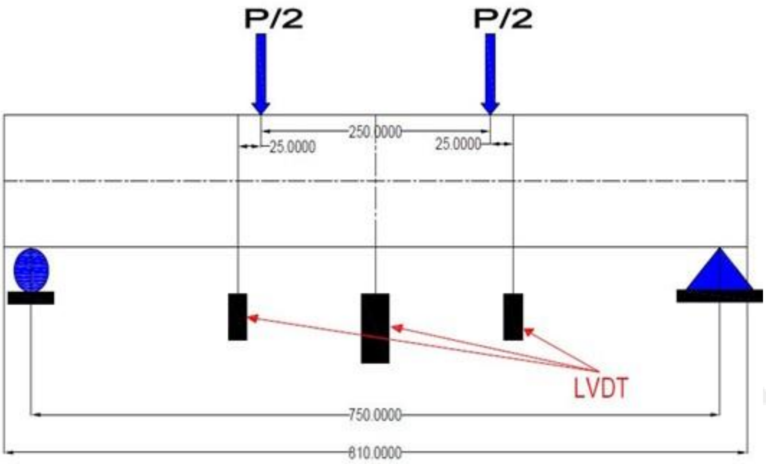

Figure 3.12 The sketch of testing details

CHAPTER IV

RESULTS AND DISCUSSIONS

In this chapter the obtained results from the test procedure are discussed and the required diagrams are drawn based on these results.

4.1 Introduction

When it was time to test, all test samples were prepared for testing. The mounted beams were loaded with equal force on the two loading points to prevent any additional load. The behavior of the reinforced concrete-coated steel (CFST) tube beams was compared with the control tube of all groups, and it was found that the bending strength of the reinforced concrete-filled steel tube beams was higher than that of the concrete-filled steel tube beam. Moreover, an important comparison between steel pipe beam filled with concrete and surrounded with reinforced concrete according to the classification of models is as follows: hollow, encased, control, and CFST beams.

4.2 Failure Modes

The testing process proceeded smoothly and strictly, and all laboratory samples behaved and failed in a long manner except forC8 and C8 samples. Failure patterns for all samples of the tested beam are shown in Figures4.1 and 4.2. Model failures in all groups can be determined as follows either by localized bending below the two loading points at the bottom edge of the notch is from the bottom, or torn if the notch is on the side, regardless of the difference in thickness of the steel tube and the difference in the diameter of the main rebar. There are instances where nothing happened during this period. There was a complete development of the CFST model without rupture. After dividing the samples into four groups, For the first group, the typical failure pattern of the first two samples tested (H8 t3 and H12 t3) showed local deformation at the two loading points on the outer surface, an external curvature was observed on the upper side of the model between the loading points, as well as cracks in many numbers on the lower side the sample.

The typical failure pattern of the second group tested samples which are (H8 t1.5 and H12 t1.5) showed local deformation at the two loading points on the outer surface as well as the appearance of buckling on the upper side of the outer beam between the loading points in the final loading stages. Also, no tensile fractures were observed on the test samples in this stage. The typical failure mode of the inner tubes in this group showed the inner buckling as a behavior of the hollow tube. The pattern of control failure was the same as that shown by other researchers such as (Han et al. 2006), (Elchalakani and Zhao, 2001), and (Tao and Han, 2004). Figures 4.1 illustrate the control failure modes and first group, respectively.

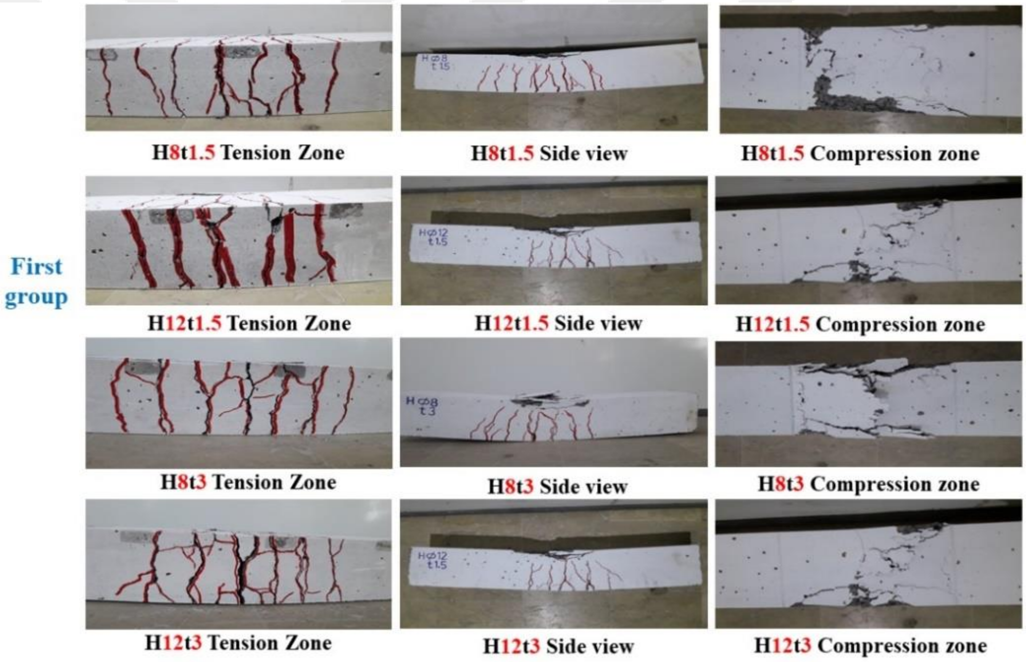

Figure 4.1 Patterns of the failures in the concrete beams (first group)

For the second group, the typical failure mode of the samples showed steel tubes filled with reinforced concrete external local curvature on the stress zone on the outside of the sample at final loading levels with local failure at the loading points on the outer surface of the steel tubes filled with reinforced concrete as it took longer to reach bending and failure.Figure 4.2 shows the failure modes of the second group.

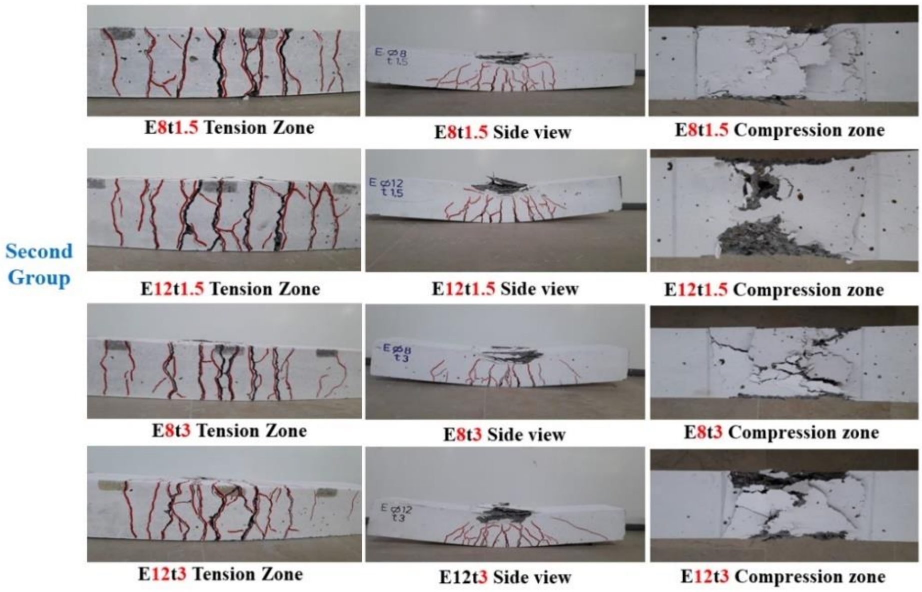

Figure 4.2 Patterns of the failures in the concrete beams (second group)

Concerning the third group, which is the concrete-filled steel tube beam. There was a complete development of the model without tearing the typical failure pattern of the two samples tested showed local deformation at the two loading points on the outer skin as well as the appearance of torsion on the upper side of the outer tube between the loading points in the final loading stages as reported in Figur 4.3. Also, no tensile fractures were observed on the test specimens at this stage. It was observed that buckling took a long time to appear in these samples.

Figure 4.3 Patterns of the failures in the concrete beams (third group)

For the two control samples, the typical failure pattern of the two samples tested showed local deformation at the two loading points on the upper outer surface. Also, an external curvature is observed on the upper side of the outer beams between the loading points. Generally, the two samples without steel tubes in the center took the shortest time to reach bending and failure. Figure 4.4 shows the failure modes of the third group.

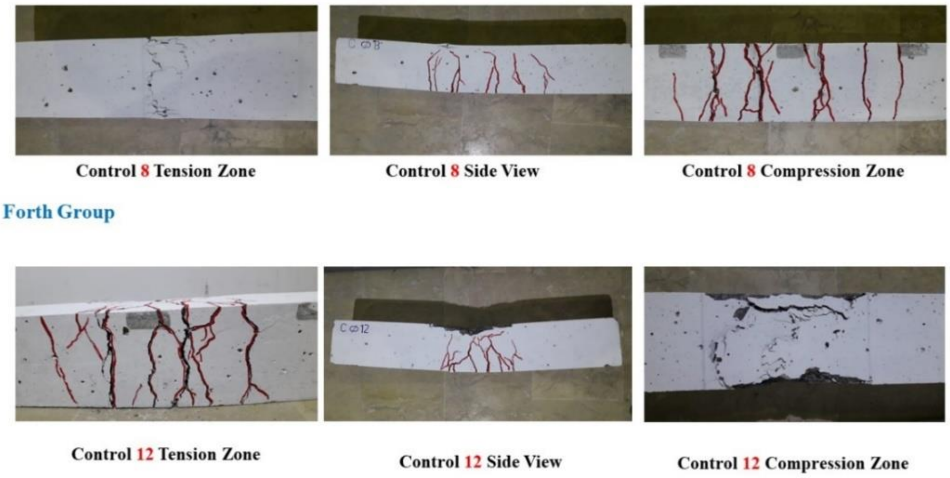

Figure 4.4 Patterns of the failures in the concrete beams (fourth group)

4.3 Moment VS Mid-Span Deflection Curves

Test results showed that all samples went through three steps of linearity, elasticity, and plasticity, in addition to showing a smooth torque deflection curve with large deflection to failure. as shown in Figure 4.5.

Figure 4.5 Deflected specimen

Control beams were compared with beams of all groups, and it was found that encased beams have a series of advantages and advantages over the control girder, such as bending stiffness, high strength, and long loading time. Also, based on steel pipe thickness and whether the beams are filled with concrete or free of concrete plus the diameter of the reinforcement. According to observations during laboratory work and load versus deflection curves, Laboratory samples showed elastic behavior in the first step of loading. Then, the curves follow an elastic path while reducing stiffness until maximum bending ability is reached. However, samples with inner tubes filled with concrete exhibit better stiffness and better bending torque ability than samples with hollow inner tubes while inner tube thickness has little effect on the medium-range instantaneous deflection curve Figures 4.6 - 4.8 illustrate the instantaneous displacement curves in the first group, the second group, and the third group samples, respectively.

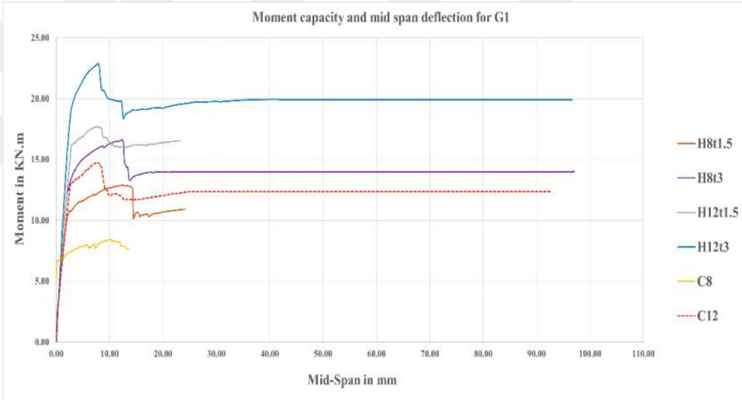

Figure 4.6 Moment vsmidspan diagram of the first group

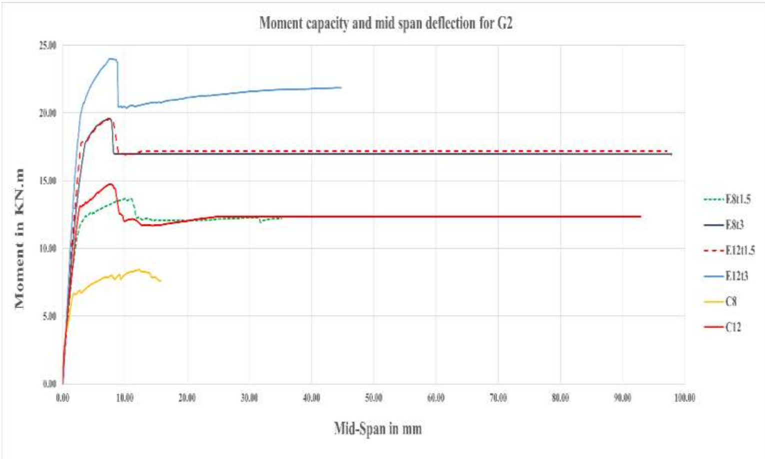

Figure 4.7 Moment vsmidspan diagram of the second group

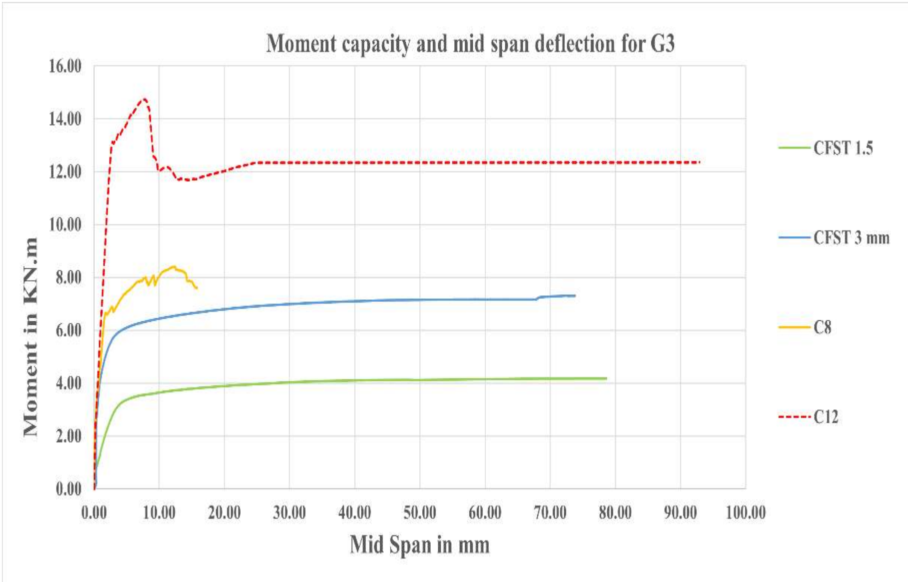

Figure 4.8 Moment vsmidspan diagram of the third group

4.4 Bending Moment Capacities

The maximum values of the experimental bending moments for all samples in all groups and the percentage increase in the instantaneous amplitude of the reinforcedconcrete-encased concrete-filled steel tubes compared to the control beams are listed in Table 4.1-4.3.

Table 4.1 Increase in moment capacity of the first group

Group name	Designation of beams	Moment Capacity (kN.m)	% Increase in Moment Capacity(kN.m)
	C12	14.74	———
First Group	E8 t1.5	13.68	7.1
	E12 t1.5	19.57	32.76
	E8 t3	19.57	32.76
	E12 t3	23.98	62.68

Table 4.2 Increase in moment capacity of the second group

Group name	Designation of beams	Moment Capacity (kN.m)	% Increase in Moment Capacity(kN.m)
	C12	14.74	____
Second Group	H8 t1.5	12.9	12.483
	H12 t1.5	17.69	20.013
	H8 t3	16.61	12.686
	H12 t3	22.88	55.223

Table 4.3 Increase in moment capacity of the third group

Group name	Designation of beams	Moment Capacity (kN.m)	% Increase in Moment Capacity(kN.m)
	C12	14.74	____
Third Group	CFST t1.5	4.17	71.709
	CFST t3	7.32	50.339

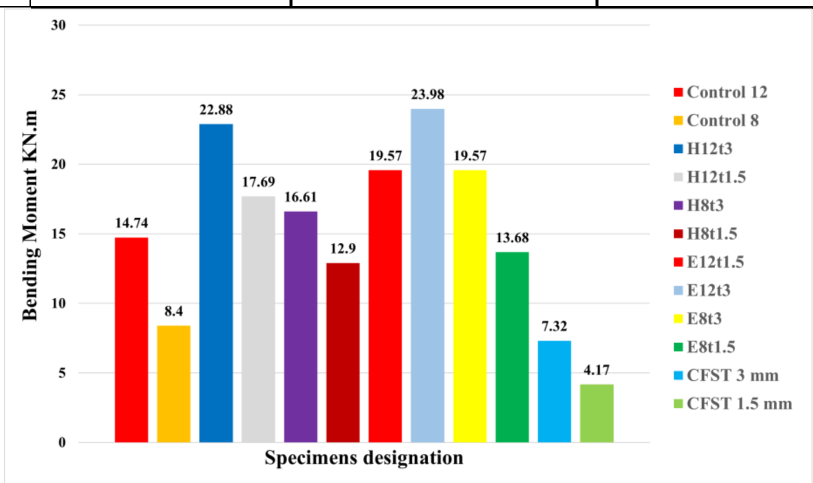

Figure 4.9 Maximum bending moment comparison among the specimens

4.5 Deflection Curves

When the loads are applied and raised gradually in beams, the response of the beams is concerning the form of the deformation. The diagrams are obtained according to the maximum value of the bending moment as shown in Figure 4.9 above. Then, the maximum moment value is multiplied by the factors (0.2, 0.4, 0.6, 0.8, 0.9, 0.96, 0.98, 0.99, and 1) to investigate the behavior of the deflection in each amount of moment. The shape of deflection is similar to the half portion of the sine wave since the beams are placed in simply supported condition and the maximum deformation occurs at the middle portion of the tested length which is (355 mm). the hollow beams. Figures 4.9 - 4.12 show the shapes of deflection for the first groupGroup, which is the hollow specimen group (Han, L. 2004).

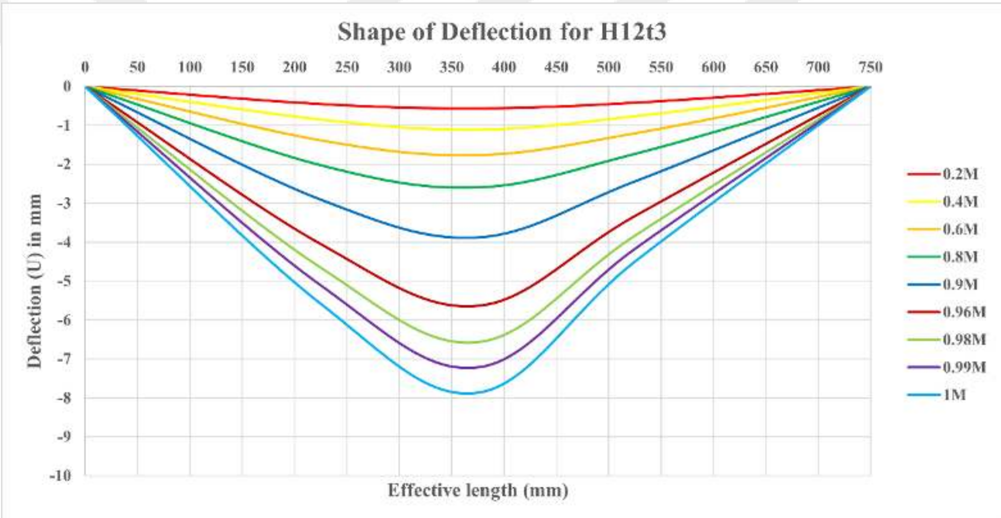

Figure 4.10 Shape of the deflection along the beam of H12t3

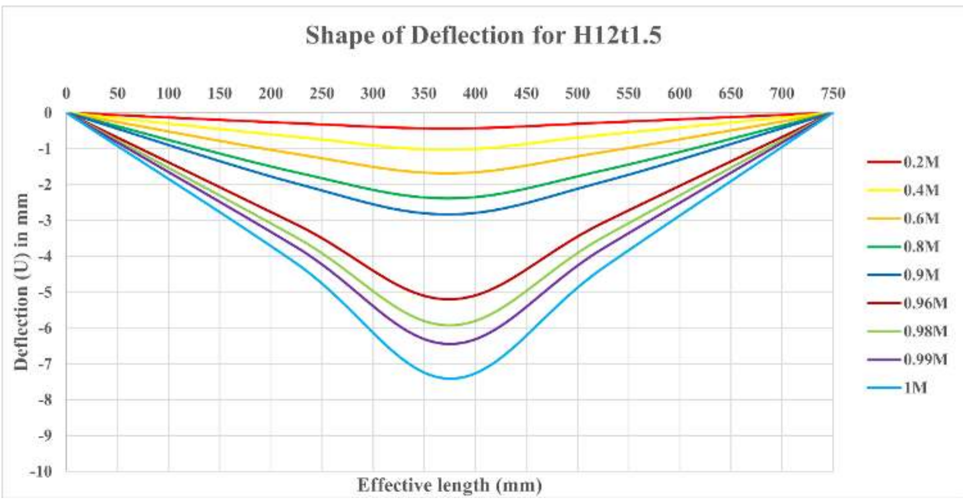

Figure 4.11 Shape of the deflection along the beam of H12t1.5

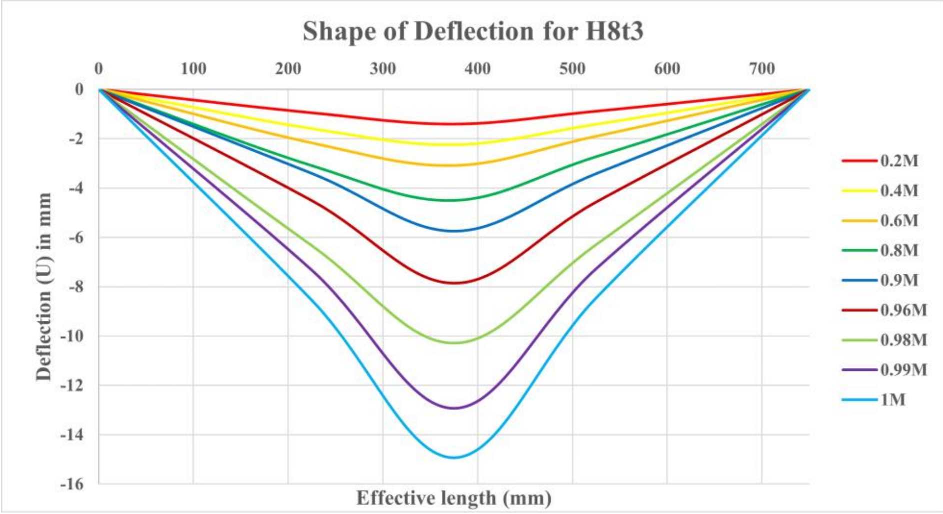

Figure 4.12 Shape of the deflection along the beam of H8t3

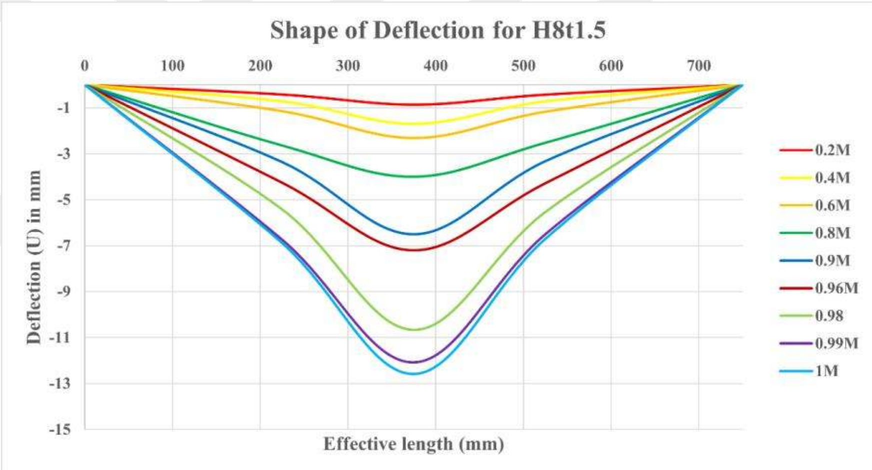

Figure 4.13 Shape of the deflection along the beam of H8t1.5

4.6 Ductility

Ductility can be defined as the ability of a material to pull or deform without tearing. Hence, it is a sign of how elastic the material is. The elasticity index of the beams was determined for all groups as shown in Figure 4.13 and Table 4.4. D_I is defined as follows:

$$D_I = \frac{D_u}{D_{0.6}} \quad \ldots\ldots\ldots\ldots\ldots\ldots\ldots\ldots\ldots\ldots\ldots\ldots\ldots\ldots\ldots\ldots\ldots\ldots\ldots\ldots\ldots\ldots\ldots(4.1)$$

Where:

D_u = displacement at the maximum moment.

$D_{0.6}$= displacement at 0.6 of the maximum moment.

Table 4.4 Ductility index for all specimens

Group name	Specimen label	D_u	D_y	D_I
Control group	C12	9.85	3.93	2.51
	C8	12.149	2.152	5.65
First group	H8 t1.5	13.586	4.089	3.32
	H12 t1.5	10.22	4.889	2.10
	H8 t3	16.271	6.273	2.59
	H12 t 3	11.988	6.9	1.74
Second group	E8 t1.5	11.482	3.775	3.04
	E12 t1.5	10.546	4.798	2.20
	E8 t3	10.546	4.798	2.20
	E12 t 3	11.602	6.02	1.93
Third group	CFST t3	62.859	4.957	12.68
	CFST t1.5	64.859	4.704	13.61

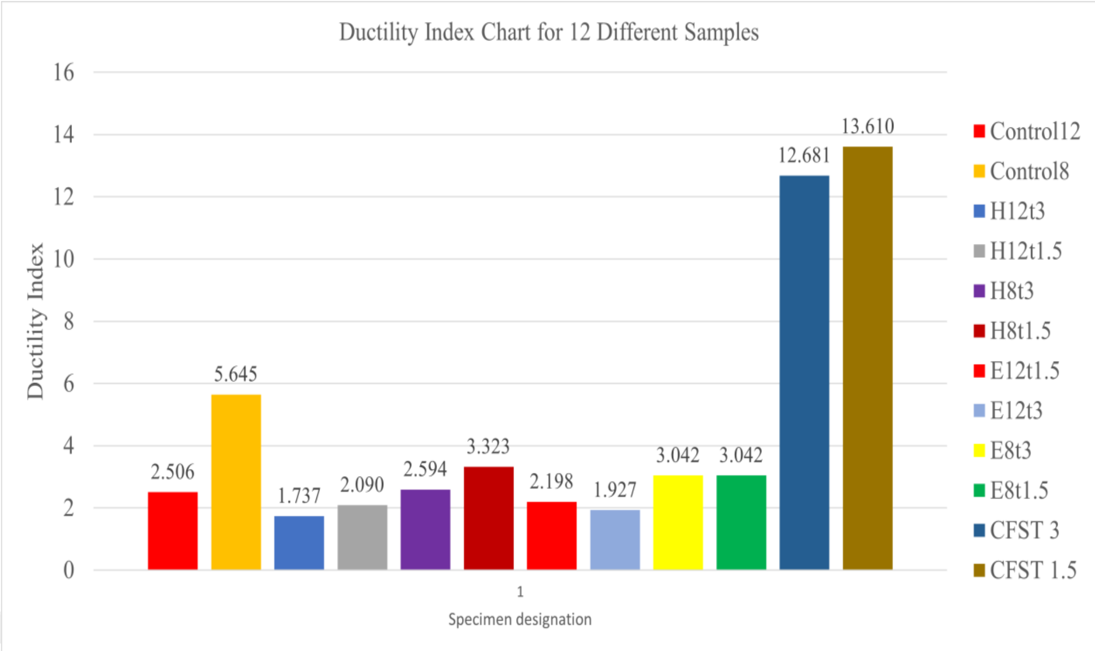

Figure 4.14 Comparison of the ductility index of all the specimens

Based on the results collected for the first group, the DI ranged from 1.74 for sample H12 t3 to 3.32 for sample H8 t1.5. Thus, the maximum DI obtained for CFST beams is 3.32 for sample H8 t1.5. For the (C8) beam, DI is 5.65 and hence, the ductility of the control beam ductility is higher than the first group.

With regards to the second group, the ductility index ranged from 1.93 for sample E12 t3 to 3.04 for sample E8 t1.5. The maximum ductility index value is 3.04 for sample H8 t1.5. Whereas for control beam DI is 5.65. The ductility of the control beam is higher than the second group.

For the third group, DI ranged from 12.68 for sample CFST t3 to 13.61 for sample CFST t1.5. The maximum DI for encased CFST beams obtained is 13.61 for sample CFST t1.5. Whereas for the control beam DI is 5.65, so the ductility of the C8 beam is less than for the third group.Based on DI, the best second group benefit was obtained. The lowest DI score was obtained in the control group.

CHAPTER V

CONCLUSION AND RECOMMENDATION

In this chapter, the obtained results are discussed according to the illustrated diagrams in chapter four and finally, the conclusions are presented briefly

5.1 Conclusions

This study focused on the performance of the encased CFST beams that were subjected to a pure bending when the outer beam shapes were of the square section while the inner tubes were of circular shapes. A comparison of encased concrete filled steel tube samples was performed based on inner tube thickness and internal reinforcing steel diameter in addition to comparing these samples to the controls The control failure mode was evident in the form of external curvature in the compression zone in addition to the occurrence of cracks and local deformation at the loading points ample. Based on the experimental results, the following conclusions may be indicated;

1. The control failure mode was evident in the form of external curvature in the compression zone in addition to the occurrence of cracks and local deformation at the loading points.
2. encased concrete filled steel tube beam failure was shown to be slightly outward curvature in the compression region plus local deformation occurred at the loading points and it took longer to reach the failure.
3. The deflection curves along the effective length at nearly different moment levels followed the sine wave curve during the entire test.
4. encased concrete filled steel tube beams showed better elastic and elastic behavior in the first stage of loading than the control beam.For the first group, the highest increase in end-moment amplitude in reinforced concrete-encased CFST beams is about 22.88 % for the sample containing a hollow concrete-

free steel inner tube as compared to the ultimate moment capacity of the control beam.

5. For the second group, the highest increase in end-moment amplitude in reinforced concrete-encased CFST beams is about 23.98% for the sample containing the concrete-filled steel tube as compared to the ultimate moment capacity of the control beam.
6. For the third group, the highest increase in the final moment amplitude of the CFST beams is about 7.32% for the sample consisting of a steel tube filled with concrete as compared to the ultimate moment capacity of the control beam.
7. For all groups, the highest significant increment in the instantaneous capacitance was obtained compared to the control samples with an inner tube filled with concrete, while the lowest increment in the ultimate moment capacity was obtained in the samples without an inner tube.

5.2 Recommendations For Future Researches

According to the previous literature, limited research has been conducted in the encased CFST. Moreover, to date, no previous study has been performed on an encased CFST beams with an inner tube in the underside of the outer tube. So that research in this field is still in its preliminary stage and more efforts are needed to fill this gap in the literature. This study relied on the use of steel inner tubes with a circular section. The thicknesses used in this study were 3 mm and 1.5 mm for the tubes. There is still a wide variety of CFST beams without various thicknesses to be used in future research. The finite element method can also be used to study the bending behavior of this type of organ. Hence, additional research is necessary to understand the behavior of encased CFST beam with different forms of tube sections.

REFERENCES

An, Y. F., Han, L. H., Roeder, C. (2014). Flexural performance of concrete-encased concrete-filled steel tubes. *Magazine of Concrete Research*, **66(5)**, 249-267.

Cai, J., Pan, J., Li, X. (2018). Behavior of ECC-encased CFST columns under axial compression. *Engineering Structures*, **171**, 1-9.

Cai, J., Pan, J., Su, H., Lu, C. (2018). Experimental study on the hysteretic behavior of ECC-encased CFST columns. *Engineering Structures*, **173**, 107-121.

Chen, J. Y., Wang, F. C., Han, L. H., Mu, T. M. (2020, October). Flexural performance of concrete-encased CFST box members. *In Structures (Vol. 27, (* ***2034-2047****). Elsevier.*

Chen, J., Chan, T. M., Chung, K. F. (2021). Design of square and rectangular CFST cross-sectional capacities in compression. *Journal of Constructional Steel Research,* **176**, 106419.

Chitawadagi, M. V., Narasimhan, M. C. (2009). Strength deformation behaviour of circular concrete filled steel tubes subjected to pure bending. *Journal of Constructional Steel Research*, **65(8-9)**, 1836-1845.

Christopher, Y., Tuan, C.Y. (2008). Flexural behavior of nonposttensioned and posttensioned concrete-filled circular steel tubes. *Journal of structural engineering,* **134(6),** 1057-1060.

Deng, Y., Tuan, C. Y., Zhou, Q., Xiao, Y. (2011). Flexural strength analysis of non-post-tensioned and post-tensioned concrete-filled circular steel tubes. *Journal of Constructional Steel Research,* **67(2),** 192-202.

El Basha, M.M. Hassan, T.K. Mohamed, M.N. Elnawawy, Omar. (2018). Efficiency of hollow reinforced concrete encased steel tube composite beams. *International Journal of Civil Engineering and Technology*. **9**. 720-735.

Elchalakani, M., Zhao, X. L., Grzebieta, R. H. (2001). Concrete-filled circular steel tubes subjected to pure bending, *Journal of Constructional Steel Research*, **57(11)**, 1141-1168.

Flor, J. M., Fakury, R. H., Caldas, R. B., Rodrigues, F. C., Araújo, A. H. M. (2017). Experimental study on the flexural behavior of large-scale rectangular concrete-filled steel tubular beams. *Revista IBRACON de Estruturas e Materiais*, **10(4)**, 895-905.

Han, L. H. (2004). Flexural behaviour of concrete-filled steel tubes. *Journal of Constructional Steel Research,* **60(2)**, 313-337.

Han, L. H., An, Y. F., Roeder, C., Ren, Q. X. (2015). Performance of concrete-encased CFST box members under bending. *Journal of Constructional Steel Research*, **106**, 138-153.

Han, L. H., An, Y. F., Roeder, C., Ren, Q. X. (2015). Performance of concrete-encased CFST box members under bending. *Journal of Constructional Steel Research,* **106**, 138-153.

Han, L. H., Lu, H., Yao, G. H., Liao, F. Y. (2006). Further study on the flexural behavior of concrete-filled steel tubes. *Journal of Constructional Steel Research*, ***62*(6)**, 554-565.

Han, L. H., Ma, D. Y., Zhou, K. (2018, June). Concrete-encased CFST structures: behaviour and application. *In Proceedings of the 12th International Conference on Advances in Steel-Concrete Composite Structures*. ASCCS 2018 **(1-10)**. Editorial UniversitatPolitècnica de València.

Lachemi, M., Hossain, K. M., Lambros, V. B. (2006). Axial load behavior of self-consolidating concrete-filled steel tube columns in construction and service stages. *ACI structural journal*, **103(1)**, 38.

Lee, H. J., Park, H. G., Kim, S. B., Park, S. S. *Flexural Capacity of Concrete-Filled Tubular Columns Encased with Precast Concrete*. Stud, 8, 240.

Li, Y. J., Han, L. H., Xu, W., Tao, Z. (2016). Circular concrete-encased concrete-filled steel tube (CFST) stub columns subjected to axial compression. *Magazine of Concrete Research*, **68(19)**, 995-1010.

Nateghi A., F., Vatandoost, M., "Seismic retrofitting RC structures with precast prestressed concrete braces ABAQUS FEA modeling", *International Journal of Engineering*, Transactions C: Aspects, **Vol. 31, No. 3**, (2018), 394-404.

Qian, W. W., Li, W., Han, L. H., Zhao, X. L. (2016). Analytical behavior of concrete-encased CFST columns under cyclic lateral loading. *Journal of Constructional Steel Research*, **120**, 206-220.

Rahmani, Z., Naghipour, M., Nematzadeh, M. (2019). Flexural performance of high-strength prestressed concrete-encased concrete-filled steel tube sections. *International Journal of Engineering*, **32(9)**, 1238-1247.

Tao, Z., Han, L. H., Zhao, X. L. (2004). Behavior of concrete-filled double skin (CHS inner and CHS outer) steel tubular stub columns and beam-columns. *Journal of Constructional Steel Research*, ***60*(8)**, 1129-1158.

Tuan, C. (2004). Aurora arch bridge. *Concrete international,* **26(4),** 64-67.

Wang, K., Luo, H. (2019). Test on Hysteretic Behaviour of Prestressed Composite Joints with Concrete-Encased CFST Columns. *Advances in Civil Engineering*, 2019.

Yang, Y., Du, X., Yu, Y., Pan, Y. (2020). Experimental study on the seismic performance of composite columns with an ultra-high-strength concrete-filled steel tube core. *Advances in Structural Engineering*, **23(4)**, 794-809.

Zhan, Y., Zhao, R., Ma, Z. J., Xu, T., Song, R. (2016). Behavior of prestressed concrete-filled steel tube (CFST) beam. *Engineering Structures,* **122,** 144-155.

Zhou, K., Han, L. H. (2018, June). Fire performance of concrete-encased CFST columns and beam-column joints. *In Proceedings of the 12th International Conference on Advances in Steel-Concrete Composite Structures*. ASCCS 2018 (**779-786).** Editorial UniversitatPolitècnica de València.

CURRICULUM VITAE

Mohammed Salah QADER

Kirkuk, Iraq

Education

- **Technical Diploma in Civil Dept. Graduated 1993.**

Technical Education of Kirkuk/Civil Dept. Iraq/ Kirkuk.

- **BSc. Civil Engineering, Graduated 2002.**

University of Baghdad/College of Engineering/ Civil Engineering. Dept. Iraq/Baghdad.

- **M.Sc. Electric and Electronic Engineering, Graduated 2021**
  University of Gaziantep College of Engineering. Civil Engineering. Dept. Gaziantep/Turkey.

Not: Currently in research stage.

JOB HISTORY

- Supervising the PANJA ALI residential project, 100 residential buildings, 50 traditional building buildings, and 50 pre-fabricated buildings- Kirkuk, Iraq, 2004 – 2009.
- Concrete casting of streets, sidewalks, and waterways, with the support of the Kurdistan Region, for the period 2007-2008 –Kirkuk, Iraq, 2007 – 2008.
- Setting up Internet towers for AL-KALEMAT Telecom Company for the period Kirkuk, Iraq, 2008-2009.
- I worked as a representative of the ARM Engineering Consulting Office to build two schools with the support of the World Bank Kirkuk, Iraq, 2008-2009
- I worked as a contractor engineer to implement 17 schools for the Kirkuk Directorate of Education Kirkuk, Iraq, 2008-2009.

- Street paving of Kiwan Military Camp for AL-MANSOUR Contracting Company Kirkuk, Iraq, 2008-2009.
- Tiling the road linking Kirkuk - Baghdad with the construction of a 980-meter bridge Kirkuk, Iraq, 2008-2009.
- Tiling the road linking Kirkuk - Baghdad with the construction of a 980-meter bridge in favor of Hammurabi Contracting Company Kirkuk, Iraq, 2008-2009.
- Construction of 20 residential houses of 200 square meters for each housing and the restoration of 13 residential homes else Kirkuk, Iraq, 2008-2009.

COMPUTER SKILLS EXPERIENCE

- Experience in the following software & programming languages:
    - Microsoft Windows (All versions).
    - Microsoft Office (All versions).
    - Microsoft Out look.
    - AutoCAD.
    - E-tabs.
    - Plan Swift.